sustainability

MDPI

Article

Functional Microbes Mediate the Impact of Soil Depth and Anthropogenic Activities on Greenhouse Gas Fluxes in the Yellow River Delta, China

Zhengxi Cai [1], Qingxuan Meng [1], Jingyu Sun [1,2,3], Xinkun Zhao [1] and Qingfeng Chen [1,*]

[1] College of Geography and Environment, Shandong Normal University, Jinan 250014, China
[2] College of Ecology, Lanzhou University, Lanzhou 730000, China
[3] Center for the Pan-Third Pole Environment, Lanzhou 730000, China
* Correspondence: chensdcn@163.com

Abstract

Coastal wetlands represent significant sources of greenhouse gases (GHGs) and serve as crucial ecological interfaces between terrestrial and marine environments, substantially contributing to global biogeochemical cycles. However, GHG emission fluxes are strongly influenced by complex anthropogenic activities, yet their underlying microbial mechanisms remain poorly understood. This study investigated seven representative human-impacted sites within the Yellow River Delta. Employing a combined approach of in vitro microcosm cultivation, molecular biology, and multivariate statistical analysis, we investigated the integrated mechanisms controlling nitrous oxide (N_2O) and methane (CH_4) fluxes, with consideration of soil depth, environmental factors, microbial communities, and functional microbes. The results indicated that significant differences in GHG fluxes among different anthropogenic activities and soil depths ($p < 0.05$). Surface soil N_2O fluxes were positive within sewage irrigation areas (20.98–35.08 mg N_2O-N m^{-2} h^{-1}) and tourism development areas (12.52–23.87 mg N_2O-N m^{-2} h^{-1}), while mariculture areas displayed negative fluxes. CH_4 fluxes were positive exclusively in natural areas (surface soil: 25.02–55.54 mg CH_4-C m^{-2} h^{-1}; deep soil: 8.38–356.68 mg CH_4-C m^{-2} h^{-1}), while other areas predominantly showed negative values (surface soil: −130.98–44.32 mg CH_4-C m^{-2} h^{-1}; deep soil: −106.16–65.24 mg CH_4-C m^{-2} h^{-1}). Furthermore, a structural equations model highlighted the pivotal role of key functional microbes in soil carbon–nitrogen cycling (e.g., nirK, nosZII, and SRB) involved in soil carbon–nitrogen cycling in negatively regulating N_2O and CH_4 fluxes. The study also revealed distinct microbial responses across diverse habitats, underscoring the significant role of Proteobacteria in wetland soil. This research enhances our understanding of GHG dynamics in coastal wetlands and provides scientific evidence and potential regulatory pathways for enhancing soil biological mitigation functions and achieving carbon neutrality and sustainability within wetland ecosystems.

Keywords: coastal wetland; greenhouse gases; sustainability; soil depth; functional microbes; anthropogenic activities

Check for updates

Academic Editor: Maria De Nobili

Received: 1 February 2026
Revised: 6 March 2026
Accepted: 9 March 2026
Published: 12 March 2026

Copyright: © 2026 by the authors. Licensee MDPI, Basel, Switzerland. This article is an open access article distributed under the terms and conditions of the Creative Commons Attribution (CC BY) license.

1. Introduction

Coastal wetlands serve as critical ecotones linking terrestrial and marine environments, disproportionately contributing to global biogeochemical cycling and supporting diverse ecological communities [1,2]. These ecosystems are particularly significant in the context of global climate change, given their substantial role in the production and consumption

of greenhouse gases (GHGs), including nitrous oxide (N_2O) and methane (CH_4) [3,4]. However, coastal wetlands are increasingly subjected to a complex suite of anthropogenic activities, including nutrient loading, altered hydrology, and habitat fragmentation, all of which can profoundly impact their biogeochemical functioning (IPCC, 2021). Elucidating the interactive effects of these activities on GHG fluxes is paramount for developing effective mitigation strategies.

The Yellow River Delta, as a typical river-controlled alluvial fan, is characterized by rapid sediment deposition and subsequent dramatic shoreline dynamics [5,6]. This has resulted in a unique wetland landscape dominated by mudflats, salt marshes, and salt-tolerant vegetation such as *Suaeda salsa* and *Phragmites australis* [7–9]. Its evolutionary trajectory exhibits distinct regional characteristics: it currently faces multiple threats, including intensified salinization, eutrophication processes, and Spartina alterniflora invasion, and the natural habitat shows a pronounced degradation trend. This distinctiveness contrasts sharply with the tide-controlled stable pattern of the Yangtze River Delta and the erosion-dominated patterns of the Pearl River Delta, where urban expansion and tidal flat reclamation are the dominant pressures. The Yellow River Delta's uniqueness in geomorphological genesis, ecological composition, and combination of stressors render it an ideal study area for elucidating coastal wetland evolution mechanisms and assessing anthropogenic disturbance effects, thereby possessing both outstanding scientific value and conservation significance.

Microbial communities, such as nitrification, denitrification, and methanogenesis, primarily mediate the production and consumption of N_2O and CH_4 in wetland soils [10–12]. The activity and composition of these microbial communities are highly responsive to a range of environmental factors, including soil moisture, salinity, redox potential, and substrate availability [13–15]. Furthermore, the vertical stratification of these factors within the soil profile creates distinct microhabitats, thereby influencing the distribution and activity of microbial functional groups at different soil depths [16–20].

Despite numerous studies investigating the impact of anthropogenic activities on GHG fluxes in coastal wetlands, many exhibit limitations. For example, Chen et al. (2024) examined the effects of nutrient loading on N_2O emissions in a coastal marsh, but their analysis focused primarily on surface soil layers (0–10 cm), overlooking the significant potential contribution from deeper soil horizons to overall emissions [21–23]. Similarly, Zhang et al. (2024) investigated the impact of land reclamation on CH_4 fluxes in a mangrove ecosystem [24–26]; however, they treated the soil profile as a homogenous unit, thus failing to account for depth-dependent variations in microbial processes and environmental conditions. Moreover, few studies have explicitly examined the interactive effects of multiple anthropogenic stressors and soil depth on the abundance, expression, and activity of key functional genes underlying N_2O and CH_4 cycling. This is a critical oversight, as the vertical distribution of microbial communities and their associated biogeochemical processes significantly influences overall GHG emissions from wetland ecosystems. Addressing this knowledge gap is essential for developing spatially explicit management strategies that consider the inherent heterogeneity of microbial processes in wetland soils. In the Yellow River Delta, coastal wetlands are subjected to a complex interplay of terrestrial inputs, marine influences, and direct anthropogenic activities [27–31]. These activities can alter soil physicochemical properties, nutrient dynamics, and microbial community structure, thereby influencing N_2O and CH_4 fluxes. Indeed, Zhao et al. (2020) demonstrated the complex and potentially contrasting effects of urbanization and soil salinization on vegetation productivity in this region, further underscoring the need for a more nuanced understanding of the factors controlling GHG emissions [32–36].

Therefore, this study aims to elucidate the impact of anthropogenic activities on N_2O and CH_4 fluxes in Yellow River Delta wetlands, with a specific focus on the role of soil depth in modulating microbial-mediated processes. We hypothesize that: (1) Anthropogenic activities will exert differential effects on N_2O and CH_4 fluxes across different soil depths, reflecting variations in soil properties and microbial community composition. (2) Specific anthropogenic activities will alter the abundance and expression of key microbial functional genes involved in N_2O and CH_4 production and consumption, and these alterations will exhibit depth-dependent patterns. (3) Shifts in microbial community structure, driven by anthropogenic activities and modulated by soil depth, will be correlated with variations in N_2O and CH_4 fluxes. By addressing these hypotheses, this study will contribute to a more nuanced understanding of the complex interactions between anthropogenic activities, soil depth, microbial processes, and GHG emissions in coastal wetlands, ultimately informing more effective management strategies for mitigating climate change.

2. Materials and Methods

2.1. Soil Samples Collection

Soil samples were collected during the summer of 2025 from six areas in the central part of the Yellow River Delta (119°9′19″–119°9′29″ E, 37°44′47″–37°46′44″ N): the Yellow River irrigation area (YA), sewerage irrigation area (SA), mariculture area (MA), oil exploitation area (OA), Yellow River water transfer area (TA) and tourism development area (LA). A natural area (CK) from the Yellow River Delta Nature Reserve, minimally impacted by anthropogenic activities, served as the control (Figure 1).

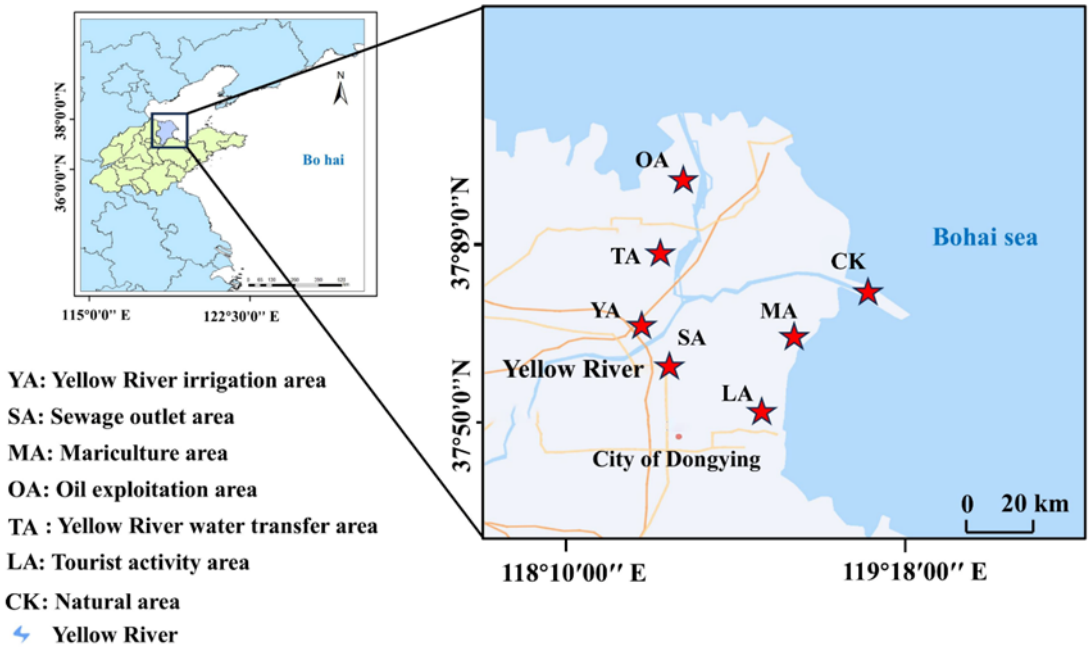


Figure 1. The sampling sites in the Yellow River Delta. The red stars represent the location of each sample. Detailed names of each sample are placed in the left corner of the figure.

The sampling timing was selected for the following reasons: First, July represents the warm season in the region, with relatively stable precipitation and higher temperatures, during which soil microbial activity and nutrient cycling are more active, thus better reflecting ecological processes under anthropogenic influences. Second, summer vegetation is lush, with increased surface litter input, helping to reveal the effects of different land-use types on the accumulation of organic matter and pollutants in surface soil. Additionally,

this period avoids the strong disturbances of spring irrigation and autumn harvesting, allowing a more accurate capture of the baseline soil properties.

After removing surface debris, three soil cores were collected from each location at 0–20 cm (surface soil) and 20–40 cm (deep soil) depths. Numbered samples were stored in self-sealing bags, refrigerated, and transported to the laboratory. Samples were divided: one part was air-dried and ground for physicochemical analysis, and the other was stored at −80 °C for molecular analysis [12].

2.2. Soil Environmental Factors

Soil pH and oxidation–reduction potential (ORP) were determined using a 1:2.5 (*w*/*v*) soil-to-water ratio [37]. Electrical conductivity (EC) was determined using a soil-to-water ratio of 1:5 (*w*/*v*) and measured as a soil salinity index [14]. Sulfate (SO_4^{2-}) level was determined with ion chromatography after a two-hour extraction with deionized water [38]. Ammonium ion (NH_4^+) and nitrate ion (NO_3^-) levels were assessed by extracting 5 g of soil in 50 mL of 2M KCl and analyzing the solution with an AA3 continuous flow analyzer (AA3, Seal Analytical, Norderstedt, Germany) [38]. To determine the nitrite ion (NO_2^-) level in the soil, we utilized the principle of diazotization of NO_2^- with sulphonamide, which was extracted with 2M KCl and measured using a spectrophotometer [39]. Total nitrogen (TN) and total carbon (TC) were determined using an elemental analyzer (FlashSmart, Elementar Analysensysteme GmbH, Langenselbold, Germany) after grinding and sieving the soil samples, following the standard combustion method to quantify the gaseous N and C emissions [39]. Soil temperature (T) was measured in situ using a portable soil thermometer (HOBO U23-001, Bourne, MA, USA) at each sampling point, with three replicates taken for each point and the average value recorded [37].

2.3. Soil Greenhouse Gases Fluxes

To isolate the soil intrinsic GHG emission potential from transient environmental fluctuations and to enable a controlled comparison across soils with distinct anthropogenic activities, a laboratory incubation experiment was conducted under standardized conditions. Briefly, 200 g of fresh soil was placed in 250 mL serum vials, which were then sealed with butyl rubber stoppers and aluminum crimp caps to minimize water loss. A three-way valve connected to the stopper via a small needle ensured gas-tight sampling. Incubation conditions matched in situ temperature, with daily humidity adjustments maintained within the microcosms. Gas samples were collected daily for 7 days. The first sample (C_0) was taken immediately, and a second sample (C_1) was taken 40 min later [39]. N_2O and CH_4 were detected using a gas chromatograph (Agilent 7890B; Agilent, Palo Alto, CA, USA) equipped with a flame ionization detector [40]. N_2O and CH_4 fluxes for each area are calculated as follows [39]:

$$GHG\ flux = \frac{(C_1 - C_0) \times HV \times P \times C_L \times M_{GHG} \times C_{mg}}{(t_1 - t_0) \times SA \times R \times T_k}$$

where GHG flux is hourly GHG emissions (mg N_2O-N m^{-2} h^{-1}; mg CH_4-C m^{-2} h^{-1}); HV is headspace volume inside the bottle (L); P is atmospheric pressure (1 atm); C_L is conversion factor µL to L (0.000001 L); M_{GHG} is molecular weight of N in N_2O and C in CH_4 (g mol^{-1}); C_{mg} is conversion factor ug to mg (1000 mg μg^{-1}); t_0 is time the first was sample taken (0 h); t_1 is time second sample was taken (0.33 h); SA is surface area of culture flask (m^2); R is the universal gas constant (0.0821 L atm $mol^{-1}K^{-1}$); and T_k is temperature (°C).

2.4. DNA Extraction, PCR Amplification, and Sequencing

Microbial DNA was extracted from approximately 0.5 g of soil samples using the Magnetic Soil and Stool DNA kit (Tiangen, China) following the manufacturer's instructions. Agarose gel electrophoresis was then performed to assess DNA purity and concentration, with appropriate amounts of the sample placed in centrifuge tubes and diluted to 1 ng μL^{-1} in sterile water.

Wetland soil DNA was analyzed by PCR amplification using bacterial universal primers 341F/806R and archaeal universal primers Arch519F/Arch915R [39], with three replicates established for each DNA sample. The PCR products were purified by electrophoresis using a 1× TAE agarose gel at a concentration of 2% according to their concentration after mixing equal amounts of PCR products, and the target bands were recovered by cutting the gel. Library construction kits (TruSeq DNA Kit, Illumina, Inc., San Diego, IL, USA) were generated using the Illumina TruSeq DNA Polymerase-Free Chain Reaction Library Preparation Kit, quantified with Qubit, and sequenced after passage with NovaSeq 6000 (Beijing, China).

2.5. Fluorescence Quantitative PCR Analysis

The abundance (i.e., copy number) of all functional genes was determined by a Roche LightCycler 480 real-time PCR system (Roche Diagnostics, Mannheim, Germany) and quantitative PCR with fluorescent SYBR dye. The primer sequences and the quantitative PCR protocols used are shown in Table S1. A standard curve was constructed using a known amount of tandem plasmid diluent containing the DNA of the standard sample plasmid.

2.6. Statistical Analysis

Statistical analyses were conducted in R software (version 4.3.1) to unravel the intricate relationships among soil physicochemical properties, microbial communities, functional genes, and gas fluxes, integrating a suite of advanced methodologies. For correlation analyses, Pearson correlation analysis was used to quantify linear associations between soil physicochemical indices, carbon–nitrogen cycling functional genes, and gas fluxes. The corrplot package in R was employed to generate heatmaps, visualizing correlation coefficients (r) and significance levels ($p < 0.05$ for significant and $p < 0.01$ for highly significant correlations). Additionally, Mantel tests, a non-parametric correlation method implemented via the vegan package, were performed to explore the relationships between functional genes and gas fluxes, where Mantel' r values ($> |0.4|$) and $p < 0.01$ indicated significant associations.

For modeling, random forest (RF) models, constructed using the random forest package, were utilized to identify key environmental predictors of gas fluxes. Mean % increase (a measure of variable importance) and mean squared error (MSE, reflecting model accuracy) were determined to rank the contributions of different factors. Structural equation modeling (SEM), executed through the lavaan package, was applied to elucidate the direct and indirect pathways through which anthropogenic activities, soil depth, environmental factors, microbial communities, and functional genes influenced N_2O and CH_4 fluxes. Model fit was assessed using the goodness-of-fit index (GFI) and *p*-values, while path coefficients (rounded to two decimal places) quantified the strength of direct effects [41,42].

In microbial community and network analyses, 3D principal component analysis (3D PCA), conducted with the FactoMineR and factoextra packages, enabled the dimensionality reduction of microbial composition data. The extracted principal components (PCs) and their variance contributions were used to reveal clustering patterns across different regions and soil layers. Co-occurrence networks, constructed via the igraph package, were analyzed to characterize microbial community complexity, with node numbers, edge counts, and

proportions of positive/negative effects used to quantify network structure and inter-taxa interactions. A consistent significance threshold of $p < 0.05$ (significant) and $p < 0.01$ (highly significant) was applied throughout all analyses, and results were reported with two decimal places for precision.

3. Results

3.1. Effects of Soil Environmental Factors on N_2O and CH_4 Fluxes

Random forest modeling and Pearson correlation analysis identified key factors influencing greenhouse gas fluxes (Figure 2). In the surface soil, nitrate, salinity and electrical conductivity were identified as significant factors. In the deep soil, nitrate, total nitrogen and electrical conductivity served as key factors. Pearson correlation analysis further revealed that in the surface soil, nitrate and SO_4^{2-} correlated significantly negatively with N_2O flux ($p < 0.001$ and $p < 0.05$), while NH_4^+ and total nitrogen correlated significantly negatively with CH_4 flux ($p < 0.01$ and $p < 0.05$). In the surface and deep soil layer, nitrate also exhibited a significant negative correlation with N_2O flux ($p < 0.05$) (Figure 2). Furthermore, total nitrogen in the surface and deep soil layers showed a negative correlation with CH_4 flux.

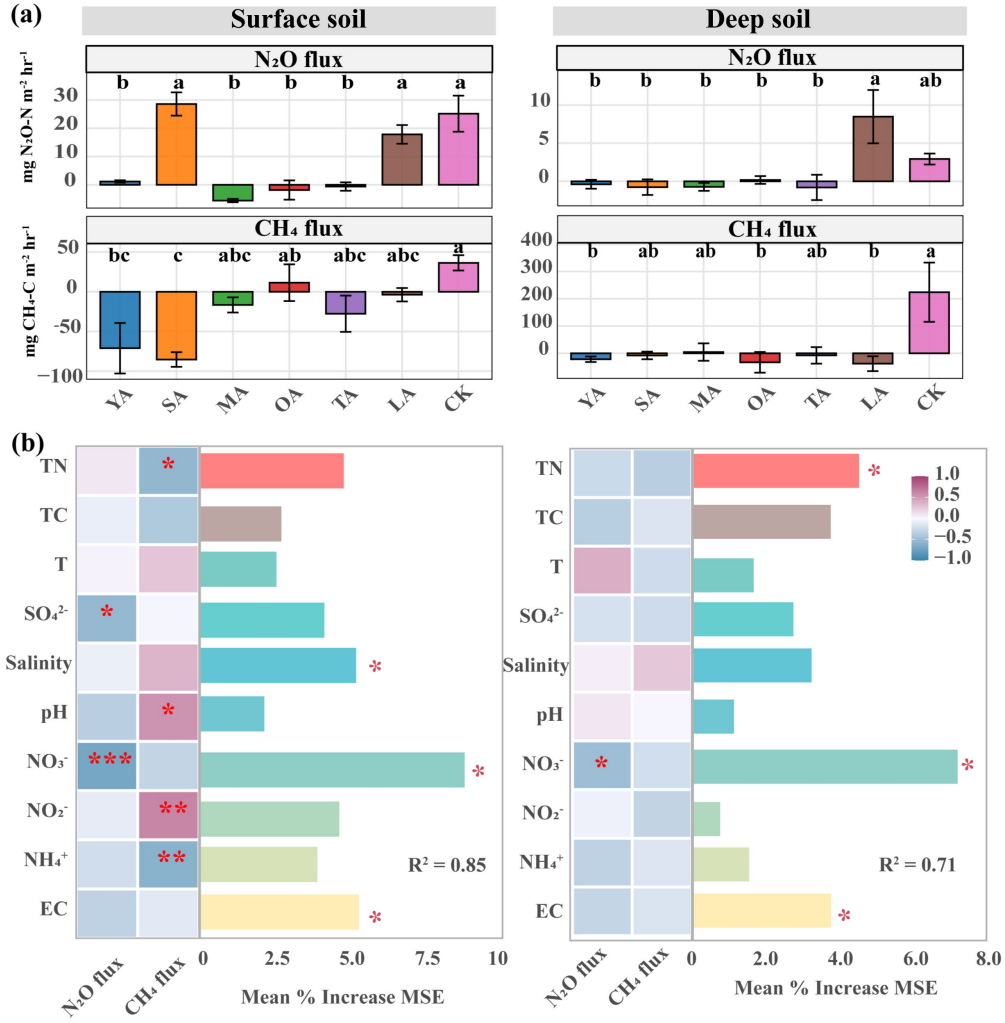


Figure 2. The influence of environmental factors on greenhouse gas fluxes. (**a**) N_2O and CH_4 gas fluxes in surface and deep soils; (**b**) RF analysis model examining relationships between soil physicochemical properties and N_2O and CH_4 gas fluxes in different soil depths, with significance levels denoted as * $p < 0.05$, ** $p < 0.01$, and *** $p < 0.001$. Different lowercase letters (a, b, c) indicate statistically significant differences between groups ($p < 0.05$).

3.2. Effects of Different Soil Depths on N_2O and CH_4 Fluxes

Environmental factors, as detailed in the Supplementary Materials, significantly affected GHG fluxes at different depths. Overall, N_2O flux was higher in surface soil than in deep soil (Figure 2). In surface soil, SA (20.98–35.08 mg N_2O-N m^{-2} h^{-1}) and LA (12.52–23.87 mg N_2O-N m^{-2} h^{-1}) exhibited relatively high N_2O fluxes, while MA (−6.69 to −4.63 mg N_2O-N m^{-2} h^{-1}) was the only region exhibiting N_2O absorption. Notably, compared to the CK (14.35–36.43 mg N_2O-N m^{-2} h^{-1}), SA exhibited a potentially similar N_2O flux. However, LA showed a potential decrease of up to 65.6% compared to CK.

In deep soil, N_2O flux decreased across all regions, with LA showing the highest value (1.71–13.40 mg N_2O-N m^{-2} h^{-1}), while MA and YA ranged from −1.62 to 0.99 mg N_2O-N m^{-2} h^{-1}. Furthermore, in contrast to CK (2.09–2.98 mg N_2O-N m^{-2} h^{-1}), SA, LA, MA, and YA all exhibited a potential decrease in N_2O flux by up to 42.6%.

Regarding CH_4 flux (Figure 2), only the CK in surface soil had all positive values (25.02–55.54 mg CH_4-C m^{-2} h^{-1}), while most other regions had negative values. In deep soil, the CH_4 flux in the CK surged to 8.38–356.68 mg CH_4-C m^{-2} h^{-1}. Importantly, compared to the CK (300.08–356.68 mg CH_4-C m^{-2} h^{-1}), SA, LA, MA, TA, and YA all showed a potential decrease in CH_4 flux of up to 111%.

3.3. The Influence of Anthropogenic Activities on Microorganisms

The soil bacterial and archaeal communities in surface and deep soil differed distinctly in composition, community assembly processes, and co-occurrence networks (Figures 3–7). For bacteria, the dominant phylum included Proteobacteria (30.45–65.75%), Gemmatimonadota (3.98–21.36%), and Acidobacteriota (2.51–23.87%), while the dominant genera were *Pseudomonas* (2.21–11.54%), *Halomonas* (1.09–9.44%), and *Woeseia* (0.87–8.71%) (Figure 3). The dominant archaeal phylum included Crenarchaeota (24.69–98.69%), Nanoarchaeota (2.96–68.74%), and Halobacterota (1.02–28.22%), with dominant genera such as *Bathyarchaeia* (1.22–78.55%), *Candidatus_Nitrosopumilus* (3.69–73.66%), and *Candidatus_Nitrososphaera* (0.85–38.98%) (Figure 4).

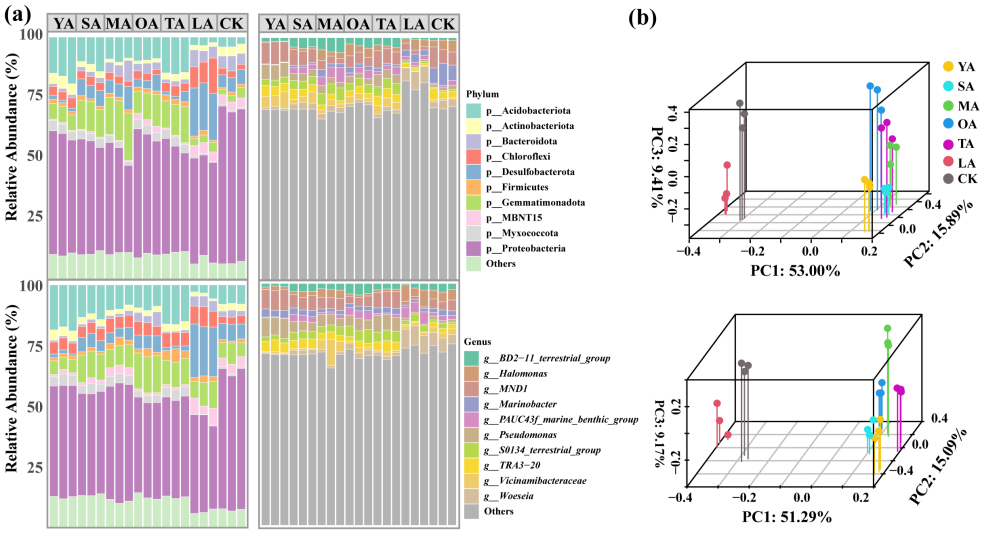


Figure 3. (**a**) Left-hand stacked bar charts display the relative abundances of soil bacteria at the phylum and genus levels across different sampling sites, with corresponding 3D PCA plots on the right (**b**).

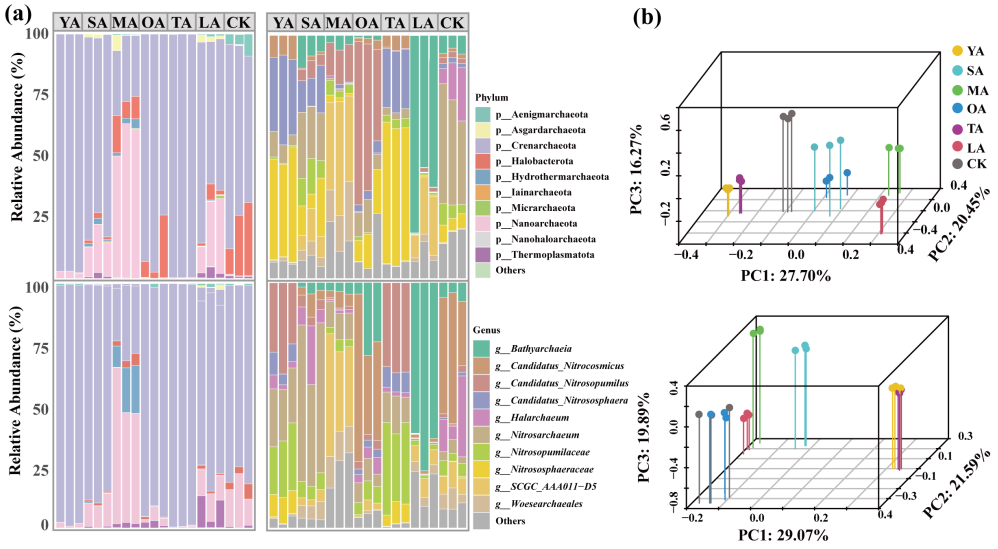


Figure 4. (**a**) Left-hand stacked bar charts display the relative abundances of soil archaea at the phylum and genus levels across different sampling sites, with corresponding 3D PCA plots on the right (**b**).

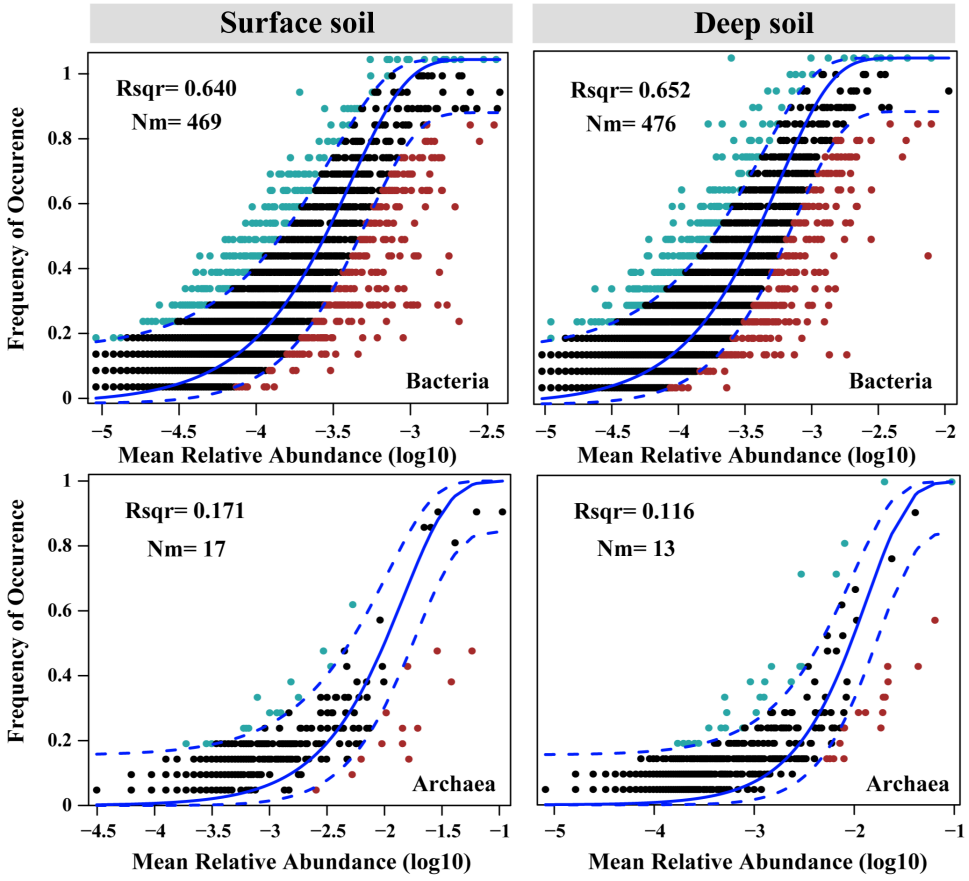


Figure 5. The neutral community analysis model of archaea and bacteria in deep and surface soil. Rsqr denotes the proportion of variation explained by the model, representing the portion of community composition attributable to neutral processes; Nm is the product of migration rate and community size, reflecting inter-community migration intensity. Red dots indicate preferred species, blue dots represent disfavored species, and black dots denote species consistent with neutral processes. The model results indicate that the explanatory power of neutral processes varies across different taxonomic groups.

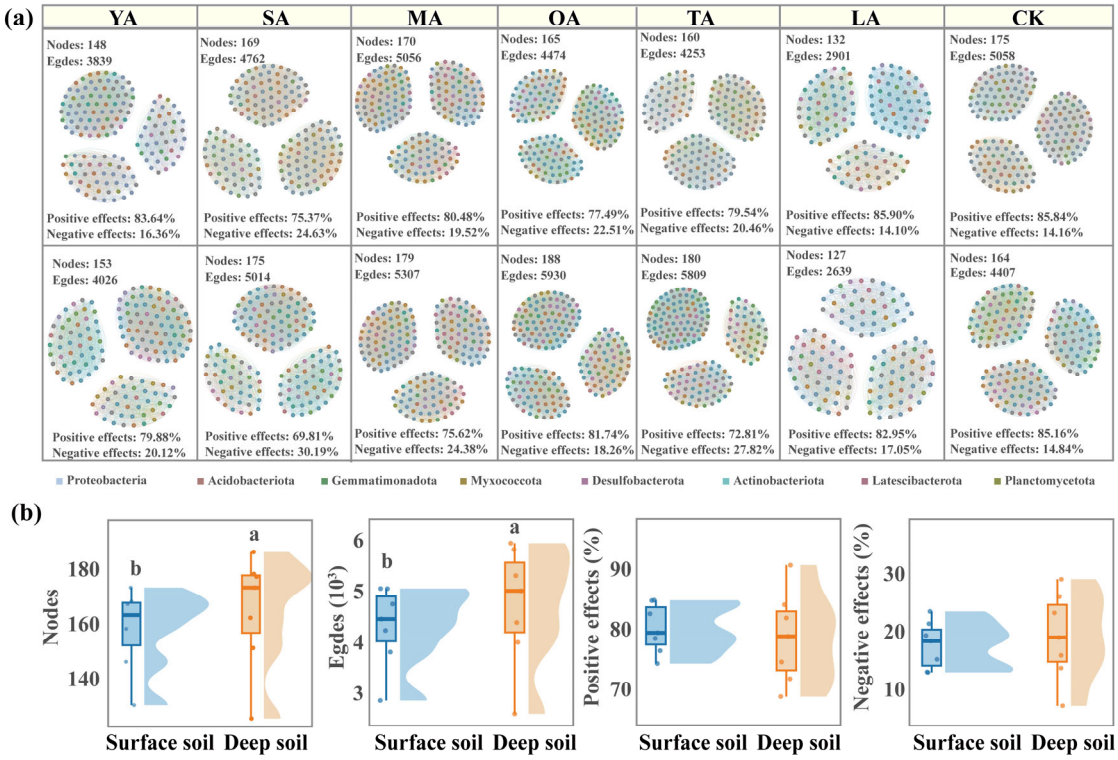


Figure 6. (**a**) Bacteria co-occurrence network under different anthropogenic activities. The upper layer is surface soil, and the lower layer is deep soil. (**b**) Scatter boxplots illustrate the number of nodes, number of edges, positive effects, and negative effects of co-occurrence networks in different soil depths.

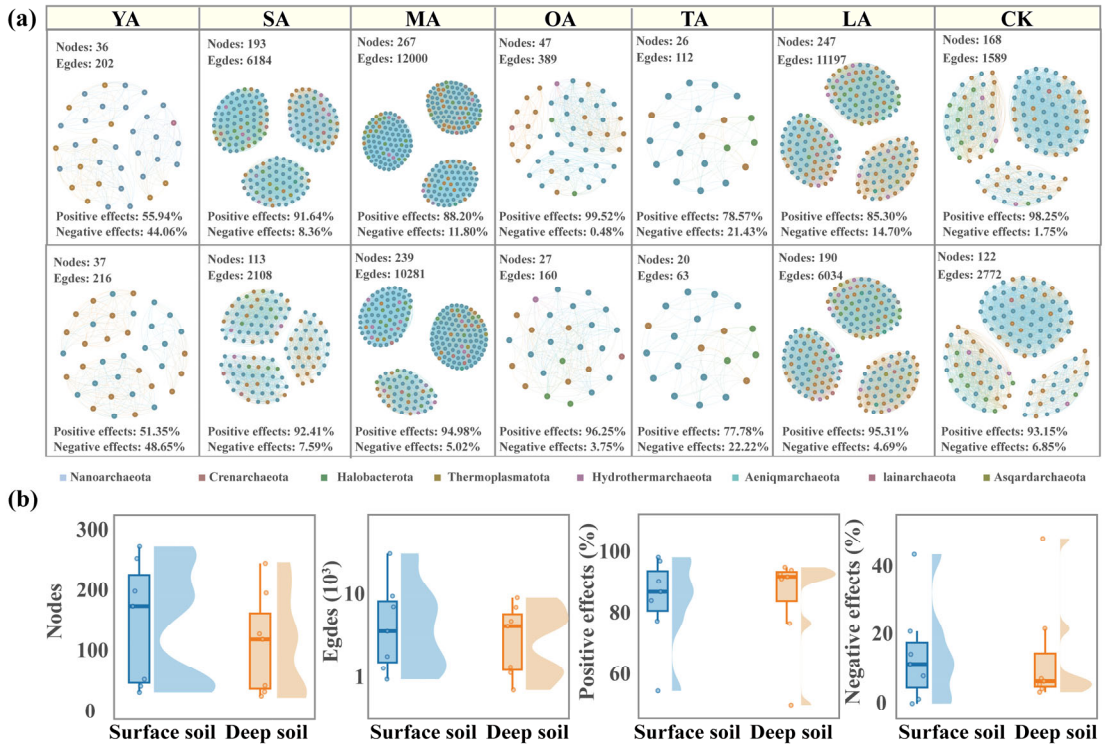


Figure 7. (**a**) Archaea co-occurrence network under different anthropogenic activities. The upper layer is surface soil, and the lower layer is deep soil. (**b**) Scatter boxplots illustrate the number of nodes, number of edges, positive effects, and negative effects of co-occurrence networks in different soil depths.

To further explore the factors driving these community differences, PCA was performed. For bacterial communities, PC1 explained 53.00% and 51.29% of the variance in surface soil and deep soil, respectively (Figure 3). For archaeal communities, PC1 explained 27.70% and 29.07% of the variance in surface soil and deep soil, respectively (Figure 4). Subsequently, community assembly processes were investigated. Bacterial communities exhibited an Rsqr of 0.640 in surface soil and 0.652 in deep soil, both higher than those observed for archaea (0.171 in surface soil and 0.116 in deep soil) (Figure 5).

Finally, to understand the interactions within these communities, co-occurrence network analysis was conducted. In surface soil, bacterial networks exhibited 132–170 nodes (10.11% less than CK) and 2901–5056 edges (16.68% less than CK), with positive effects comprising 75.37–85.90% (6.33% less than CK). In deep soil, these networks exhibited 127–188 nodes (1.83% higher than CK) and 2639–5930 edges (8.63% higher than CK), with positive effects comprising 69.81–85.16% (9.42% less than CK) (Figure 6). The number of nodes and edges in the bacterial network of the deep soil layer was significantly higher than that in the surface soil ($p < 0.05$) (Figure 6). In surface soil, archaeal networks exhibited 26–267 nodes (19.05% less than CK) and 112–12,000 edges (14.48 times CK), with positive effects accounting for 78.57–99.52% (15.32% less than CK) (Figure 7). In deep soil, these networks exhibited 20–239 nodes (14.48% less than CK) and 63–10,281 edges (13.41% higher than CK), with positive effects accounting for 77.78–96.25% (9.25% less than CK). The number of nodes, edges, positive effects, and negative effects in surface soil did not significantly differ from those in the deep soil ($p > 0.05$) (Figure 7).

3.4. Effects of Soil Functional Genes on N_2O and CH_4 Fluxes

The Mantel test revealed correlations between carbon–nitrogen cycling functional genes and GHGs (Figure 8). In surface soil, amoA and amoB positively correlated with N_2O flux (Mantel' $r > 0.4$, $p < 0.05$). Conversely, nirK, nosZII, and SRB negatively correlated with N_2O flux (Mantel' $r > 0.4$, $p < 0.05$). Furthermore, mcrA strongly positively correlated with CH_4 flux (Mantel' $r > 0.6$, $p < 0.01$). In contrast, SRB, ANME, NC10 bacteria, and narG negatively correlated with CH_4 flux (Mantel' $r > 0.4$, $p < 0.05$).

Similarly, in deep soil, narG, nirK, and nirS were positively correlated with N_2O flux (Mantel' $r > 0.4$, $p < 0.05$). However, ANME and nosZI significantly negatively correlated with N_2O flux (Mantel' $r > 0.4$, $p < 0.05$). Additionally, mcrA strongly positively correlated with CH_4 flux (Mantel' $r > 0.6$, $p < 0.01$). Finally, ANME and narG were significantly negatively correlated with CH_4 flux (Mantel' $r > 0.4$, $p < 0.05$).

3.5. Path Analysis of Factors Influencing Soil N_2O and CH_4 Fluxes

This SEM (Figure 9) elucidated the influence paths and contributions of different factors on N_2O and CH_4 fluxes through path analysis. Anthropogenic activities positively impacted key environmental factors (path coefficient = 0.615). Depth negatively impacted key microorganisms (path coefficient = −0.687) and key environmental factors (path coefficient = −0.666). Key environmental factors positively impacted network positive effects (path coefficient = 0.587) and key microorganisms (path coefficient = 0.777), key microorganisms had a significant positive impact on key functional genera (path coefficient = 0.811), and key functional genus ultimately exerted a significant negative impact on N_2O flux (path coefficient = −0.852) and CH_4 flux (path coefficient = −0.897). The total effects plot showed differences in the contributions of various factors to N_2O and CH_4 flux. Key functional genus exhibited the highest negative total effects to N_2O and CH_4 fluxes (−1.211 and −1.744).

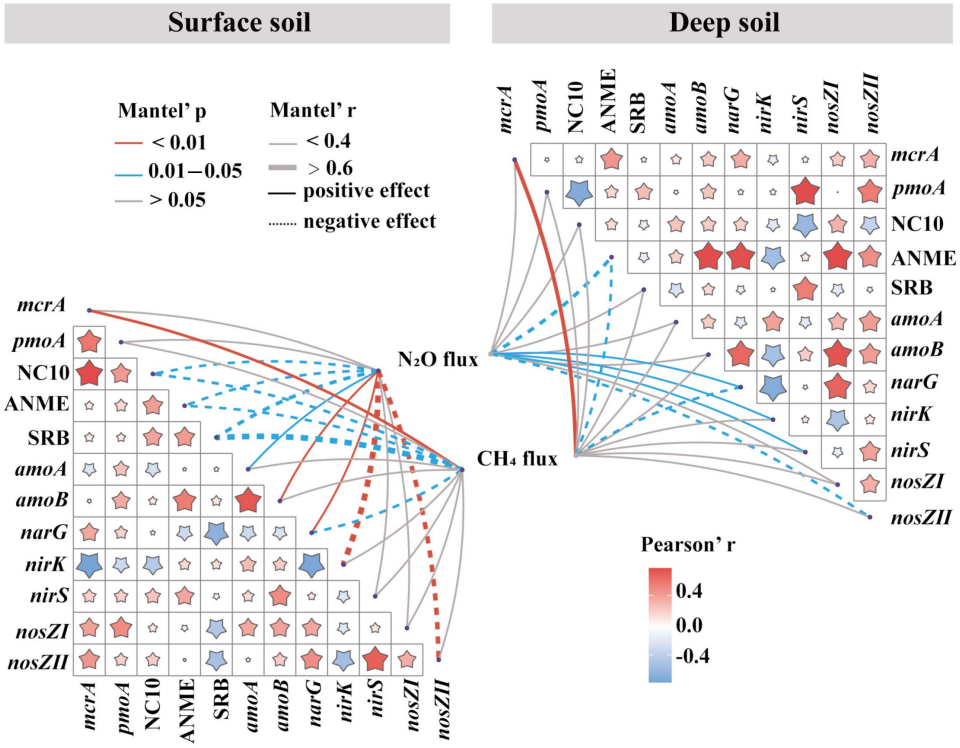


Figure 8. The Mantel's test evaluated the relationship between soil functional microbial genes and N_2O and CH_4 fluxes. The depth of color and size within each five-pointed star indicate the strength of the correlation. Solid lines represent positive correlations, and dashed lines represent negative correlations. Red lines indicate $p < 0.01$, and blue lines indicate $p < 0.05$. The thickness of the lines is proportional to the correlation coefficient.

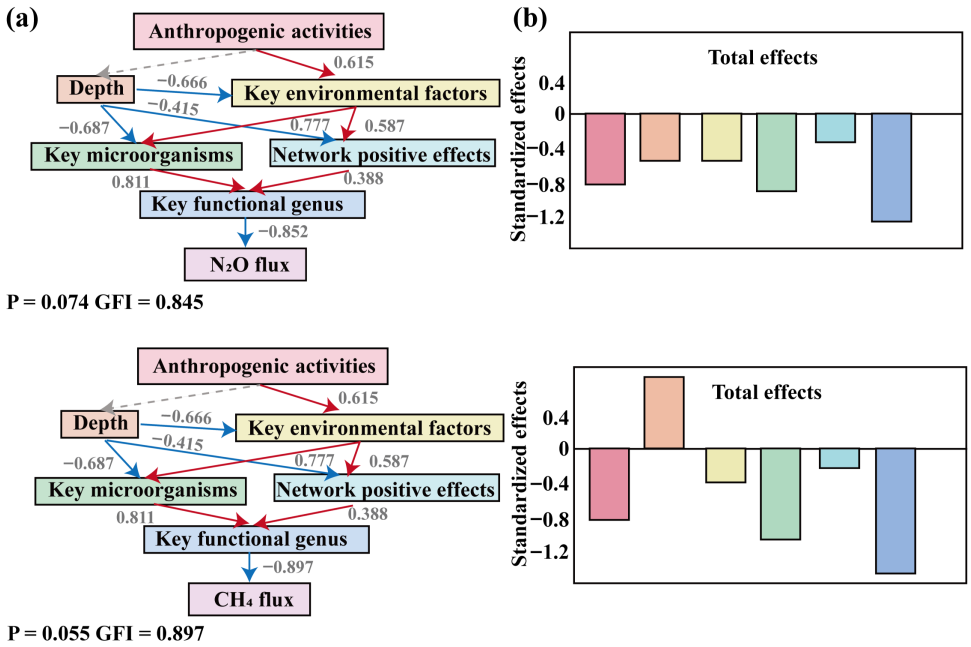


Figure 9. (**a**) SEM depicts the unidirectional influence paths of various factors in coastal wetlands under the impact of human activities and the standardized effect values. Red arrows indicate positive correlations, blue arrows indicate negative correlations, and gray dashed lines indicate no significant correlations. The R value quantifies the proportion of the variation effect derived from SEM. Total effects (combining direct and indirect effects) derived from SEM are presented, the colors of the bar charts in the total effects diagram correspond one-to-one with the color blocks representing different factors in the SEM structural equation (**b**).

4. Discussion

4.1. Effects of Soil Depth on Microbial Greenhouse Gas Fluxes

Soil depth emerges as a critical determinant of microbial community structure and function within the Yellow River Delta, thereby profoundly influencing greenhouse gas fluxes across habitats subjected to varying anthropogenic pressures. This study specifically investigated the effects of soil depth on microbial communities and their functions, with a particular focus on N_2O and CH_4 fluxes across different anthropogenic activity areas in the Yellow River Delta. By examining the intricate interactions between habitat type and soil depth, this research aims to provide novel insights into the complex dynamics of microbial communities within this unique ecosystem and their consequential contribution to greenhouse gas emissions.

Regarding habitat specificity, high-salinity marine aquaculture systems, being directly anthropogenically modified, exert the most pronounced influence on microbial communities. Within surface soils, the prevailing saline environment fosters archaeal communities, predominantly composed of the phylum Halobacteria [43–45], which actively metabolize and deplete substantial organic carbon. This depletion of organic carbon consequently suppresses nitrification–denitrification microbial activity, resulting in the surface layer uniquely exhibiting N_2O uptake. This phenomenon is consistent with established reports of high salinity inhibiting denitrification [46–48]. However, with increasing depth, the complexity of the archaeal network diminishes while denitrifying bacteria become progressively enriched. This compositional shift leads to a transition in deep-layer N_2O flux to shift from uptake to low emissions. This thus addresses a critical research gap concerning the depth-dependent evolution of microbial functions in hypersaline environments. This functional transition may be attributed to specific functional gene expression during denitrification; for instance, the upregulation of the nitrous oxide reductase gene nosZ in deep soils may promote N_2O conversion to N_2, thereby mitigating emissions. Consequently, it is inferred that the upregulation of the nosZ gene in the deep layers of the marine aquaculture area plays a crucial role in diminishing N_2O emissions.

In stark contrast, the unique characteristics of sewage treatment zones stem from human waste discharge. Specifically, surface soils in these areas, having absorbed substantial domestic sewage, exhibit elevated NH_4^+ concentrations. This nutrient enrichment fosters the proliferation of bacterial communities dominated by the Proteobacteria phylum [49–51], thereby leading to markedly higher N_2O fluxes in surface soils compared to other areas. Conversely, with increasing soil depth, the vertical transport of sewage substrates diminishes, leading to a reduction in NH_4^+ concentrations and concomitant shifts in bacterial community composition. Taken together, these depth-dependent variations in microbial communities and their functions within the sewage treatment area underscore the pivotal role of substrate availability and other environmental factors in regulating anthropogenic soil greenhouse gas emissions.

This finding revises the previous notion that microbial function in sewage-affected areas is solely substrate-controlled [40], indicating depth-mediated substrate attenuation as a key regulatory factor. In contrast, the depth-dependent response of microbial communities in natural reed beds provides a benchmark for understanding how human activities disrupt natural processes. In surface soils, reed rhizosphere exudates provide abundant carbon sources for bacteria and archaea [37], forming a synergistic metabolic network that promotes nitrification and N_2O production. With increasing depth, the decomposition of reed residues elevates total carbon content [14], leading to methanogen enrichment and a surge in mcrA gene expression. This, in turn, substantially increases deep methane flux, consistent with reports of heightened methane production in deep wetlands [39]. Concurrently, increased moisture in the sub-surface soil creates anaerobic microenviron-

ments, potentially triggering anaerobic methane oxidation involving methanogens [42], illustrating the complexity of these processes [52,53]. By comparing with other habitats, this study posits that the deep accumulation of reed residues is the core natural factor driving anomalous methane emissions, providing new evidence for distinguishing between anthropogenic and natural microbial functional impacts. Moreover, hydrological variations and nutrient inputs from surrounding farmland may influence these 'natural' systems, whilst human-disturbed soils may exhibit lower greenhouse gas fluxes due to key microorganisms either not producing gases or actively reducing emissions [54].

High N_2O fluxes in the surface layer of sewage areas may be driven by ammonia-oxidizing bacteria (containing the amoA gene) and denitrifying bacteria (containing the nirK/nirS genes), with incomplete denitrification under anoxic conditions readily leading to N_2O accumulation. Although the surge in mcrA gene expression in the deep layer of the reed zone indicates enhanced methane production, anaerobic methane oxidation mediated by anaerobic methanotrophs (ANME) and sulphate-reducing bacteria (SRB) may also occur in the anaerobic microenvironment. The functional gene expression and relative activity of these organisms will ultimately determine the net methane flux in this layer.

In summary, soil depth significantly influences microbial communities in the Yellow River Delta and their impact on greenhouse gas fluxes. Human activities further alter this relationship. The nirK and nosZII genes respectively encode the key enzymes nitrite reductase (nirK) and nitrous oxide reductase (nosZII) within the denitrification pathway. Together, they determine the capacity of microorganisms to produce and consume N_2O, constituting the core molecular mechanism regulating soil N_2O gas flux. Surface soils in marine aquaculture exhibit salinity-driven archaeal dominance and potential N_2O reduction regulation. Sewage input promotes Proteobacteria growth and elevated N_2O fluxes. Methane production increases in the deep soil of reed wetlands. These findings underscore the necessity of considering depth-dependent microbial dynamics when assessing greenhouse gas emissions from coastal ecosystems, particularly under anthropogenic influences.

4.2. Influence of Anthropogenic Activities on Microbial Community Structure

This study departs from the traditional, often fragmented, understanding of soil GHG flux regulation, which has conventionally emphasized individual factors [37,42,55]. We hypothesized that a more holistic approach, one that comprehensively integrates the complex interplay of soil depth, environmental conditions, microbial community structure, and functional gene expression, would be essential for unraveling the drivers of N_2O and CH_4 emissions in disturbed ecosystems.

In light of this hypothesis, we employed SEM to construct a novel 'soil depth–environmental factors–microbial community–functional genes–gas flux' coupling pathway in the multi-disturbed Yellow River Delta. This innovative framework enabled us to transcend simple correlations, thereby facilitating the quantification of both the direct and indirect effects of key variables on N_2O and CH_4 fluxes.

The SEM analysis revealed a clear mechanist pathway for both N_2O and CH_4 fluxes, thereby underscoring the central role of key functional genes. Anthropogenic activities exerted a significant positive impact on key environmental factors, thus establishing them as a primary driver of alterations in soil conditions. Soil depth, conversely, on the other hand, had a significant negative impact on both key microorganisms and key environmental factors, indicating that deeper soil layers are associated with distinct microbial communities and consequently modified environmental conditions.

These key environmental factors, in turn, had significant positive impacts on both network positive effects and key microorganisms, thereby demonstrating the importance of environmental conditions in shaping microbial community structure and interactions.

Key microorganisms subsequently exerted a significant positive impact on key functional genera, further emphasizing the role of microbial communities in driving the abundance and activity of specific functional genes. Crucially, these key functional genera ultimately had a significant negative impact on both N_2O flux and CH_4 flux. This unequivocally indicates that the abundance and activity of these key functional genes are directly linked to the attenuation of both N_2O and CH_4 emissions. Further corroborating these findings, the Mantel test revealed a negative correlation between nirK, nosZII, and SRB genes and N_2O flux in the surface soil. This observation strongly suggests their pivotal role in N_2O reduction via denitrification and dissimilatory nitrate reduction to ammonium.

The positive correlation between amoA and amoB and N_2O flux in the surface soil strongly implies that nitrification may also serve as a significant pathway for N_2O production in this specific environment. It is important to note that the specific functional genes that are driving the reduction in N_2O and CH_4 emissions likely vary depending on the habitat and environmental conditions. For example, in the reed wetland, the pmoA gene, which encodes for particulate methane monooxygenase, may be highly expressed in methanotrophs, consequently leading to a substantial increase in CH_4 oxidation. This is consistent with the observation of positive CH_4 flux values in the CK of surface soil, which are indicative of vigorous methanotrophic activity.

While the overall mechanistic pathway was consistent for both gases, the total effects analysis revealed differences in the relative contributions of various factors to N_2O and CH_4 fluxes. Notably, key functional genes exhibited the highest negative total effects on both N_2O and CH_4 fluxes, thereby unequivocally reinforcing their central role in mitigating GHG emissions. This finding underscores the critical importance of understanding and promoting the activity of these key functional genes, which is crucial for effective GHG mitigation strategies. Specifically, strategic interventions aimed at enhancing denitrification, DNRA, and methanotroph activity could be promising avenues for reducing GHG emissions in this ecosystem.

The habitat-specific observations further enrich our understanding by providing essential context for how this overall pathway manifests in diverse environments. For example, in the sewage discharge outlet, the high nitrogen input may be a primary driver of shifts in microbial community composition, favoring organisms that harbor the key functional genes responsible for N_2O reduction. Similarly, in the mariculture area, the influence of salinity on microbial community structure may be a crucial factor affecting the abundance and activity of key functional genes involved in CH_4 oxidation. The reed area, with its high organic carbon content, may be fostering a microbial community that is particularly effective at utilizing these key functional genes to reduce both N_2O and CH_4 emissions. These observations underscore the importance of considering habitat-specific management strategies for GHG mitigation.

These habitat-specific observations align with previous studies highlighting the roles of pH and salinity as key factors controlling ammonia-oxidizing and methane-oxidizing microorganisms in sediments [54,56,57]. For instance, Nitrosarchaeum, a dominant AOA taxon in coastal wetlands, exhibits a 'salt-in' effect to maintain osmotic balance in hypersaline conditions [58,59], while amoB and Nitrosomonas play crucial roles in CH_4 oxidation, contributing to the suppression of CH_4 emissions [60–62]. Our findings corroborate these previous studies and further emphasize the importance of environmental factors in shaping microbial community structure and function.

The negative correlation between ANME and narG and CH_4 flux in the deep soil further supports the idea that AOM and denitrification may play a role in regulating CH_4 emissions in these environments. The expression levels of these functional genes are likely influenced by a complex interplay of environmental factors, including pH, salinity,

and the availability of electron donors and acceptors. Future studies should investigate the specific environmental controls on AOM and denitrification in the deep soil of the Yellow River Delta.

In conclusion, this study provides a novel framework for understanding the complex interplay of soil depth, environmental conditions, microbial communities, and functional genes in regulating GHG fluxes in the Yellow River Delta. Future research should focus on further elucidating the specific functional genes involved in GHG cycling and their regulation by environmental factors in different habitats. Furthermore, exploring the potential for manipulating environmental conditions to promote the activity of beneficial functional genes could offer promising strategies for mitigating GHG emissions in coastal wetlands.

4.3. Research Limitations and Future Prospects

This study successfully revealed soil-depth-driven microbial community changes and their regulatory mechanisms on greenhouse gas fluxes under different anthropogenic activities in the Yellow River Delta. However, several limitations warrant discussion.

First, greenhouse gas fluxes were exclusively measured using in vitro culture experiments. Although this method allows for the control of environmental variables and precise analysis of microbial metabolic processes, laboratory conditions inherently diverge significantly from in situ field environments. Specifically, the controlled temperature, humidity, and substrate supply during cultivation may not fully replicate the complex physicochemical conditions of field soil, which could consequently compromise the accurate assessment of certain microorganisms, particularly strict anaerobes like methanogens, and also impact methanotroph activity. Therefore, it is imperative that future research should integrate field in situ flux observations to validate the ecological relevance of laboratory findings.

Second, sampling in this study was conducted exclusively at a single time point, thereby lacking seasonal dynamic monitoring data. The Yellow River Delta, situated in a temperate monsoon climate zone, experiences pronounced seasonal variations, including alternating dry and wet seasons, temperature fluctuations, and vegetation phenological characteristics that may significantly influence microbial community structure and function. For instance, high temperatures and humidity in summer may enhance methanogen activity, whereas seasonal droughts in spring and autumn may suppress denitrification processes. Sampling at a single time point inevitably precludes capturing these temporal dynamics, consequently limiting the accuracy of estimating annual greenhouse gas emissions. Subsequent studies should conduct long-term, season-spanning observations at fixed locations to comprehensively reveal the temporal variability of microbially driven greenhouse gas fluxes.

Furthermore, while this study primarily focused on the effects of soil depth and anthropogenic activity type on microbial communities, it did not systematically evaluate potential confounding effects arising from spatial heterogeneity in hydrological connectivity, vegetation type, and soil physicochemical properties. Future research is therefore encouraged to integrate high-resolution spatial sampling with multivariate statistical analysis to more precisely clarify the relative contributions of these environmental factors.

Nevertheless, despite these acknowledged limitations, this study provides a crucial theoretical foundation for understanding the mechanisms of microbial-driven greenhouse gas emissions in coastal wetlands under human disturbance and effectively paves the way for subsequent research.

5. Conclusions

This study explored the intricate regulatory mechanisms governing N_2O and CH_4 fluxes across seven distinct habitats within the Yellow River Delta through a series of indoor

microcosm experiments. It examined soil environmental factors, microbial communities, and functional genes, with a particular emphasis on the dynamic differences observed between surface and deep soil. The key findings are as follows:

The regulation of greenhouse gas fluxes by soil environmental factors exhibited significant depth-dependent variations. In the surface soil, nitrate and SO_4^{2-} significantly inhibited N_2O fluxes, whereas NH_4^+ and total nitrogen markedly suppressed CH_4 fluxes. Conversely, in the deep soil, nitrate and total nitrogen emerged as the key inhibitory factors for N_2O and CH_4 fluxes, respectively. N_2O fluxes exhibited pronounced vertical differentiation and spatial heterogeneity. Notably, emission intensities were relatively low in marine aquaculture areas, where high salinity promoted archaeal dominance and facilitated N_2O uptake (N_2O flux: -6.69 to -4.63 mg N_2O-N m^{-2} h^{-1}), potentially through the inhibition of denitrification. Microbial community structure and co-occurrence networks varied with depth, with more complex bacterial interactions observed at the seabed. Key functional genes, including amoA, nirK/S, and mcrA, showed direct correlations with gas fluxes, and their activity patterns were depth-regulated. SEM indicates that anthropogenic activities regulate N_2O (-0.852) and CH_4 (-0.897) fluxes via a 'environmental factors–microbial communities–functional genes–gas fluxes' pathway, underscoring the enhancement of specific functional microbial communities as a central biological mechanism for suppressing greenhouse gas emissions.

Research indicates that modulating key functional genes such as nirK, nosZII, and SRB can effectively reduce N_2O emissions, providing novel targets for greenhouse gas mitigation strategies. Our findings suggest targeted strategies should be implemented in the Yellow River Delta region to reduce greenhouse gas emissions: prioritizing nitrogen emission reduction in high-emission areas such as sewage treatment zones while promoting the development of greenhouse gas mitigation functional genes; prudently managing salinity in marine aquaculture to avoid inhibiting denitrification; implementing soil management practices to foster healthy microbial communities and enhance greenhouse gas reduction functional genes. Further research is required to validate causal relationships and identify additional factors influencing greenhouse gas emissions. These actions will contribute to reducing greenhouse gas emissions and safeguarding the ecological integrity of the Yellow River Delta.

Supplementary Materials: The following supporting information can be downloaded at: https://www.mdpi.com/article/10.3390/su18062798/s1, Figure S1: Environmental factors in surface soils under different anthropogenic activities, Figure S2: Environmental factors in deep soils under different anthropogenic activities, Figure S3: Distribution of functional genes in surface soils under different anthropogenic activities, Figure S4: Distribution of functional genes in deep soils under different anthropogenic activities, Figure S5: The correlation correlation between Alpha diversity and GHG(N_2O, CH_4) fluxs at different soil depths, Figure S6: Summary of co-occurrence network parameter supplement; Table S1: Supplementary table.

Author Contributions: Z.C.: Conceptualization, Formal analysis, Investigation, Methodology, Data curation, Writing—original draft. Q.M.: Data curation, Supervision. J.S.: Methodology. Formal analysis, Data curation, Writing—original draft. X.Z.: Funding acquisition. Q.C.: Supervision, Writing—review and editing, Funding acquisition. All authors have read and agreed to the published version of the manuscript.

Funding: The research was funded by the National Natural Science Foundation of China (42077051), the Natural Science Foundation of Shandong Provincial (ZR2025MS576), and the Taishan Scholars Young Experts of Shandong Province (TSQN201812086).

Data Availability Statement: Data will be made available on request.

Acknowledgments: We are grateful to Yingxue Sun and Chengxiu Lu from the College of Geography and Environment, Shandong Normal University, for their support in the instrument analysis. Special thanks to Beijing Novogene Technology Co., Ltd. for technical assistance with the molecular work.

Conflicts of Interest: The authors declare that they have no known competing financial interests or personal relationships that could have appeared to influence the work reported in this paper.

References

1. Bedi, M.; Sapozhnikova, Y.; Taylor, R.B.; Ng, C. Per- and polyfluoroalkyl substances (PFAS) measured in seafood from a cross-section of retail stores in the United States. *J. Hazard. Mater.* **2023**, *459*, 132062. [CrossRef] [PubMed]
2. Bi, R.; Xu, X.; Zhan, L.; Chen, A.; Zhang, Q.; Xiong, Z. Proper organic substitution attenuated both N_2O and NO emissions derived from AOB in vegetable soils by enhancing the proportion of Nitrosomonas. *Sci. Total Environ.* **2023**, *866*, 161231. [CrossRef] [PubMed]
3. Cui, S.H.; Liu, P.F.; Guo, H.A.; Nielsen, C.K.; Pullens, J.W.M.; Chen, Q.; Pugliese, L.; Wu, S.B. Wetland hydrological dynamics and methane emissions. *Commun. Earth Environ.* **2024**, *5*, 470. [CrossRef]
4. Du, X.; Deng, Y.; Li, S.; Escalas, A.; Feng, K.; He, Q.; Wang, Z.; Wu, Y.; Wang, D.; Peng, X.; et al. Steeper spatial scaling patterns of subsoil microbiota are shaped by deterministic assembly process. *Mol. Ecol.* **2021**, *30*, 1072–1085. [CrossRef]
5. Fan, G.; Zhang, D.; Zhang, J.; Li, Z.; Sang, W.; Zhao, L.; Xu, M. Ecological environmental effects of Yellow River irrigation revealed by isotope and ion hydrochemistry in the Yinchuan Plain, Northwest China. *Ecol. Indic.* **2022**, *135*, 108574. [CrossRef]
6. Fang, C.; Liu, K.-d.; Tian, F.-j.; Li, J.-y.; Li, S.-j.; Zhang, R.-m.; Sun, J.; Fang, L.-x.; Ren, H.; Wang, M.-g.; et al. Metagenomic analysis unveiled the response of microbial community and antimicrobial resistome in natural water body to duck farm sewage. *Environ. Pollut.* **2024**, *361*, 124784. [CrossRef]
7. Wu, L.; Chen, X.M.; Wei, W.; Liu, Y.W.; Wang, D.B.; Ni, B.J. A Critical Review on Nitrous Oxide Production by Ammonia-Oxidizing Archaea. *Environ. Sci. Technol.* **2020**, *54*, 9175–9190. [CrossRef]
8. Xu, H.H.; Deng, Y.P.; Zou, J.; Zhang, K.M.; Li, X.Y.; Yang, Y.H.; Huang, S.Q.; Liu, Z.Q.; Wang, Z.; Hu, C. Nitrification performance and bacterial community dynamics in a membrane bioreactor with elevated ammonia concentration: The combined inhibition effect of salinity, free ammonia and free nitrous acid on nitrification at high ammonia loading rates. *Sci. Total Environ.* **2022**, *831*, 154972. [CrossRef]
9. Liu, B.; Hou, L.; Zheng, Y.; Zhang, Z.; Tang, X.; Mao, T.; Du, J.; Bi, Q.; Dong, H.; Yin, G.; et al. Dark carbon fixation in intertidal sediments: Controlling factors and driving microorganisms. *Water Res.* **2022**, *216*, 118381. [CrossRef]
10. Gu, X.; Wang, T.; Li, C. Elevated ozone decreases the multifunctionality of belowground ecosystems. *Glob. Change Biol.* **2023**, *29*, 890–908. [CrossRef]
11. Hristov, A.N.; Melgar, A.; Wasson, D.; Arndt, C. Symposium review: Effective nutritional strategies to mitigate enteric methane in dairy cattle. *J. Dairy Sci.* **2022**, *105*, 8543–8557. [CrossRef] [PubMed]
12. Wei, G.; Li, M.; Shi, W.; Tian, R.; Chang, C.; Wang, Z.; Wang, N.; Zhao, G.; Gao, Z. Similar drivers but different effects lead to distinct ecological patterns of soil bacterial and archaeal communities. *Soil Biol. Biochem.* **2020**, *144*, 107759. [CrossRef]
13. Wen, B.; Zhang, X.L.; Yang, Z.P.; Xiong, H.G.; Qiu, Y. Influence of tourist disturbance on soil properties, plant communities, and surface water quality in the Tianchi scenic area of Xinjiang, China. *J. Arid. Land* **2016**, *8*, 304–313. [CrossRef]
14. Khatri, N.; Tyagi, S. Influences of natural and anthropogenic factors on surface and groundwater quality in rural and urban areas. *Front. Life Sci.* **2015**, *8*, 23–39. [CrossRef]
15. Li, X.E.; Hou, Y.L.; Chu, X.J.; Zhao, M.L.; Wei, S.Y.; Song, W.M.; Li, P.G.; Wang, X.J.; Han, G.X. Ambient precipitation determines the sensitivity of soil respiration to precipitation treatments in a marsh. *Glob. Change Biol.* **2023**, *29*, 2301–2312. [CrossRef]
16. Liu, C.; Shan, Y.; Wang, Q.; Harris, P.; Liu, Y.; Wu, L. Impacts of measured soil hydraulic conductivity on the space-time simulations of water and nitrogen cycling. *Catena* **2023**, *226*, 107058. [CrossRef]
17. Long, Y.C.; Jiang, J.; Hu, X.J.; Hu, J.; Ren, C.G.; Zhou, S.Q. The response of microbial community structure and sediment properties to anthropogenic activities in Caohai wetland sediments. *Ecotoxicol. Environ. Saf.* **2021**, *211*, 111936. [CrossRef]
18. Ma, L.; Jiang, X.; Liu, G.; Yao, L.; Liu, W.; Pan, Y.; Zuo, Y. Environmental Factors and Microbial Diversity and Abundance Jointly Regulate Soil Nitrogen and Carbon Biogeochemical Processes in Tibetan Wetlands. *Environ. Sci. Technol.* **2020**, *54*, 3267–3277. [CrossRef]
19. Mutschlechner, M.; Praeg, N.; Illmer, P. The influence of cattle grazing on methane fluxes and engaged microbial communities in alpine forest soils. *FEMS Microbiol. Ecol.* **2018**, *94*, fiy019. [CrossRef]
20. Niu, Y.H.; Zheng, Y.L.; Hou, L.J.; Gao, D.Z.; Chen, F.Y.; Pei, C.Y.; Dong, H.P.; Liang, X.; Liu, M. Microbial dynamics and activity of denitrifying anaerobic methane oxidizers in China's estuarine and coastal wetlands. *Sci. Total Environ.* **2022**, *806*, 150425. [CrossRef]

21. Chen, M.J.; Li, W.Y.; Teng, H.B.; Hu, W.X.; Dong, Z.Q.; Zhang, D.W.; Liu, T.Y.; Zheng, Q. Impact of Combined Pollution of Ciprofloxacin and Copper on the Diversity of Archaeal Communities and Antibiotic-Resistance Genes. *Antibiotics* **2024**, *13*, 734. [CrossRef] [PubMed]
22. Pan, H.; Feng, H.; Liu, Y.; Lai, C.-Y.; Zhuge, Y.; Zhang, Q.; Tang, C.; Di, H.; Jia, Z.; Gubry-Rangin, C.; et al. Grazing weakens competitive interactions between active methanotrophs and nitrifiers modulating greenhouse-gas emissions in grassland soils. *ISME Commun.* **2021**, *1*, 74. [CrossRef] [PubMed]
23. Qiu, Q.Y.; Ding, C.; Mgelwa, A.S.; Feng, J.G.; Lei, M.; Gan, Z.Y.; Zhu, B.; Hu, Y.L. Contrasting impacts of fertilization on topsoil and subsoil greenhouse gas fluxes in a thinned Chinese fir plantation. *J. Environ. Manag.* **2024**, *359*, 121055. [CrossRef] [PubMed]
24. Zhang, L.; Yang, J.S.; Ge, A.H.; Xie, W.P.; Yao, R.J.; Wang, X.P. Salinity drives niche differentiation of soil bacteria and archaea in Hetao Plain, China. *J. Environ. Manag.* **2024**, *370*, 122977. [CrossRef]
25. Shen, H.; Zhang, Q.; Bi, R.; Xu, X.; Zhang, X.; Fan, C.; Xiong, Z. Linkages of nitrogen-cycling microbial resistance and resilience to soil nutrient stoichiometry under dry-rewetting cycles with different fertilizations and temperatures in a vegetable field. *Sci. Total Environ.* **2022**, *820*, 153294. [CrossRef]
26. Shen, L.; Wu, L.; Wei, W.; Yang, Y.; MacLeod, M.J.; Lin, J.; Song, G.; Yuan, J.; Yang, P.; Wu, L.; et al. Marine aquaculture can deliver 40% lower carbon footprints than freshwater aquaculture based on feed, energy and biogeochemical cycles. *Nature Food* **2024**, *5*, 615–624. [CrossRef]
27. Shi, J.W.; Yang, L.; Liao, Y.; Li, J.W.; Jiao, S.; Shangguan, Z.P.; Deng, L. Soil labile organic carbon fractions mediate microbial community assembly processes during long-term vegetation succession in a semiarid region. *iMeta* **2023**, *2*, e142. [CrossRef]
28. Shi, Y.; Liu, X.; Zhang, Q.; Gao, P.; Ren, J. Biochar and organic fertilizer changed the ammonia-oxidizing bacteria and archaea community structure of saline-alkali soil in the North China Plain. *J. Soils Sediments* **2020**, *20*, 12–23. [CrossRef]
29. Shi, Y.; Ma, Q.X.; Kuzyakov, Y.; Sheng, L.X.; Liu, H.Y.; Wang, Z.Q. Nitrite-dependent anaerobic oxidation decreases methane emissions from peatlands. *Soil Biol. Biochem.* **2023**, *178*, 108658. [CrossRef]
30. Song, K.; Senbati, Y.; Li, L.; Zhao, X.L.; Xue, Y.P.; Deng, M. Distinctive Microbial Processes and Controlling Factors Related to Indirect N_2O Emission from Agricultural and Urban Rivers in Taihu Watershed. *Environ. Sci. Technol.* **2022**, *56*, 4642–4654. [CrossRef]
31. Tian, Y.; Schindlbacher, A.; Malo, C.U.; Shi, C.; Heinzle, J.; Kengdo, S.K.; Inselsbacher, E.; Borken, W.; Wanek, W. Long-term warming of a forest soil reduces microbial biomass and its carbon and nitrogen use efficiencies. *Soil Biol. Biochem.* **2023**, *184*, 109109. [CrossRef]
32. Zhao, M.; Han, G.; Li, J.; Song, W.; Qu, W.; Eller, F.; Wang, J.; Jiang, C. Responses of soil CO_2 and CH_4 emissions to changing water table level in a coastal wetland. *J. Clean. Prod.* **2020**, *269*, 122316. [CrossRef]
33. Tripathi, B.M.; Kim, M.; Tateno, R.; Kim, W.; Wang, J.; Lai-Hoe, A.; Ab Shukor, N.A.; Rahim, R.A.; Go, R.; Adams, J.M. Soil pH and biome are both key determinants of soil archaeal community structure. *Soil Biol. Biochem.* **2015**, *88*, 1–8. [CrossRef]
34. Wang, C.L.; Li, W.M.; Liu, J.; Kuzyakov, Y.; Fan, M.S.; Chen, H.Q. Soil profile greenhouse gas concentrations and fluxes from a semiarid grassland and a cropland site in an agro-pastoral ectone of northern China. *Soil Tillage Res.* **2023**, *232*, 105747. [CrossRef]
35. Wang, J.Q.; Zhao, Y.X.; Zhou, M.; Hu, J.J.; Hu, B.L. Aerobic and denitrifying methanotrophs: Dual wheels driving soil methane emission reduction. *Sci. Total Environ.* **2023**, *867*, 161437. [CrossRef]
36. Wang, X.L.; Cao, A.X.; Zhao, G.Z.; Zhou, C.B.; Xu, R. Microbial community structure and diversity in a municipal solid waste landfill. *Waste Manag.* **2017**, *66*, 79–87. [CrossRef]
37. Hu, Y.-K.; Liu, X.-Y.; He, N.-P.; Pan, X.; Long, S.-Y.; Li, W.; Zhang, M.-Y.; Cui, L.-J. Global patterns in leaf stoichiometry across coastal wetlands. *Glob. Ecol. Biogeogr.* **2021**, *30*, 852–869. [CrossRef]
38. Qin, H.L.; Tang, Y.F.; Shen, J.L.; Wang, C.; Chen, C.L.; Yang, J.; Liu, Y.; Chen, X.B.; Li, Y.; Hou, H.J. Abundance of transcripts of functional gene reflects the inverse relationship between CH_4 and N_2O emissions during mid-season drainage in acidic paddy soil. *Biol. Fertility Soils* **2018**, *54*, 885–895. [CrossRef]
39. Segarra, K.E.A.; Comerford, C.; Slaughter, J.; Joye, S.B. Impact of electron acceptor availability on the anaerobic oxidation of methane in coastal freshwater and brackish wetland sediments. *Geochim. Cosmochim. Acta* **2013**, *115*, 15–30. [CrossRef]
40. Xu, X.Y.; Liu, Y.W.; Singh, B.P.; Yang, Q.; Zhang, Q.C.; Wang, H.L.; Xia, Z.D.; Di, H.J.; Singh, B.K.; Xu, J.M.; et al. NosZ clade II rather than clade I determine in situ N_2O emissions with different fertilizer types under simulated climate change and its legacy. *Soil Biol. Biochem.* **2020**, *150*, 107974. [CrossRef]
41. Wang, X.X.; Xiao, X.M.; Zhang, X.; Wu, J.H.; Li, B. Rapid and large changes in coastal wetland structure in China's four major river deltas. *Glob. Change Biol.* **2023**, *29*, 2286–2300. [CrossRef] [PubMed]
42. Zheng, M.Y.; Qi, X.J.; Liu, Z.Y.; Wang, Y.T.; Ren, Y.B.; Li, Y.; Zhang, Y.; Chai, B.F.; Jia, T. Microbial taxonomic diversity and functional genes mirror soil ecosystem multifunctionality in nonferrous metal mining areas. *J. Hazard. Mater.* **2025**, *492*, 138149. [CrossRef]
43. Sun, J.Y.; Xu, X.Y.; Zhao, X.K.; Chen, Q.F. Multi-factor analysis of enzyme activities under anthropogenic influence in the coastal wetland of the Yellow River Delta, China. *J. Environ. Manag.* **2025**, *392*, 126811. [CrossRef] [PubMed]

44. Menegat, S. The geography of conventional agriculture's unsustainability. *Nat. Clim. Change* **2025**, *15*, 20–21. [CrossRef]
45. Mo, Y.; Du, M.; Cui, S.; Wang, H.; Zhao, X.; Zhang, M.; Li, J. Simultaneously enhancing degradation of refractory organics and achieving nitrogen removal by coupling denitrifying biocathode with MnOx/Ti anode. *J. Hazard. Mater.* **2021**, *402*, 123467. [CrossRef]
46. Yang, Y.; Li, T.; Pokharel, P.; Liu, L.; Qiao, J.; Wang, Y.; An, S.; Chang, S.X. Global effects on soil respiration and its temperature sensitivity depend on nitrogen addition rate. *Soil Biol. Biochem.* **2022**, *174*, 108814. [CrossRef]
47. Wang, Y.X.; dela Cruz, T.E.E.; Jacob, J.K.S.; Geisen, S. Species-specific impact of protists in controlling litter decomposition. *Soil Biol. Biochem.* **2024**, *199*, 109598. [CrossRef]
48. Yang, P.; Tang, K.W.; Tong, C.; Lai, D.Y.F.; Zhang, L.; Lin, X.; Yang, H.; Tan, L.; Zhang, Y.; Hong, Y.; et al. Conversion of coastal wetland to aquaculture ponds decreased N_2O emission: Evidence from a multi-year field study. *Water Res.* **2022**, *227*, 119326. [CrossRef]
49. Yu, G.; Jin, D.; Zhang, F.; Tian, S.; Zhou, Z.; Ren, Z. Extraction-adsorption coupled desulfurization of fuel oil by novel functionalized porous liquids. *Chem. Eng. J.* **2023**, *453*, 139935. [CrossRef]
50. Liao, H.H.; Yu, K.; Duan, Y.H.; Ning, Z.G.; Li, B.R.; He, L.Y.; Liu, C.X. Profiling microbial communities in a watershed undergoing intensive anthropogenic activities. *Sci. Total Environ.* **2019**, *647*, 1137–1147. [CrossRef]
51. Spivak, A.C.; Sanderman, J.; Bowen, J.L.; Canuel, E.A.; Hopkinson, C.S. Global-change controls on soil-carbon accumulation and loss in coastal vegetated ecosystems. *Nat. Geosci.* **2019**, *12*, 685–692. [CrossRef]
52. Zhao, X.K.; Sun, J.Y.; Liu, C.M.; Zhang, E.Y.; Zhao, G.L.; Chen, Q.F. Mechanisms of plant-derived and microbial residue carbon in coastal wetland soils in response to salinity gradients. *Catena* **2025**, *256*, 109108. [CrossRef]
53. Alves, R.J.E.; Wanek, W.; Zappe, A.; Richter, A.; Svenning, M.M.; Schleper, C.; Urich, T. Nitrification rates in Arctic soils are associated with functionally distinct populations of ammonia-oxidizing archaea. *ISME J.* **2013**, *7*, 1620–1631. [CrossRef] [PubMed]
54. Wang, Z.; Tang, K.; Struik, P.C.; Ashraf, M.N.; Zhang, T.; Zhao, Y.; Wu, R.; Jin, K.; Li, Y. Alteration of microbial carbon and nitrogen metabolism within the soil metagenome with grazing intensity at semiarid steppe. *J. Environ. Manag.* **2023**, *347*, 119078. [CrossRef] [PubMed]
55. Tan, L.S.; Ge, Z.M.; Zhou, X.H.; Li, S.H.; Li, X.Z.; Tang, J.W. Conversion of coastal wetlands, riparian wetlands, and peatlands increases greenhouse gas emissions: A global meta-analysis. *Glob. Change Biol.* **2020**, *26*, 1638–1653. [CrossRef] [PubMed]
56. Zheng, X.; Zhou, C.; Wu, F.; Xu, H.; Zhao, Z.; Han, Z.; Zhang, H.; Yang, S. Enhanced removal of organic, nutrients, and PFCs in the iron-carbon micro-electrolysis constructed wetlands: Mechanism and iron cycle. *Chem. Eng. J.* **2023**, *457*, 141174. [CrossRef]
57. Sun, Y.; Su, Y.; Zhao, Z.; Zhao, J.; Ye, M.; Wen, X. Capacitive heavy metal ion removal of 3D self-supported nitrogen-doped carbon-encapsulated titanium nitride nanorods via the synergy of faradic-reaction and electro-adsorption. *Chem. Eng. J.* **2022**, *443*, 136542. [CrossRef]
58. Sun, J.Y.; Xu, X.Y.; Wang, Z.H.; Li, K.; Liu, C.M.; Li, C.; Cai, Z.X.; Zhao, X.K.; Xu, X.Y.; Di, H.J.; et al. Effects of anthropogenic activities on soil microbial communities and greenhouse gas fluxes in coastal wetlands of the Yellow River Delta, China. *J. Environ. Sci.* **2026**, *161*, 176188. [CrossRef]
59. Zhuang, Q.; Shao, Z.; Li, D.; Huang, X.; Cai, B.; Altan, O.; Wu, S. Unequal weakening of urbanization and soil salinization on vegetation production capacity. *Geoderma* **2022**, *411*, 115712. [CrossRef]
60. Fang, K.; Liu, T.; Tian, G.; Sun, W.; You, X.; Wang, X. Assessing the stereoselective bioactivity and biotoxicity of penthiopyrad in soil environment for efficacy improvement and hazard reduction. *J. Hazard. Mater.* **2024**, *480*, 136476. [CrossRef]
61. Zhong, S.; Hou, B.; Zhang, J.; Wang, Y.; Xu, X.; Li, B.; Ni, J. Ecological differentiation and assembly processes of abundant and rare bacterial subcommunities in karst groundwater. *Front. Microbiol.* **2023**, *14*, 1111383. [CrossRef]
62. Zhu, Y.; Chen, G.; Yu, D.; Liu, R.; Chen, X.; Yang, Z.; Yao, T.; Gong, Y.; Shan, Y.; Wang, Y. Sludge composting with self-produced carbon source by phosphate buffer coupled hyperthermophilic pretreatment realizing nitrogen retention. *Chem. Eng. J.* **2023**, *476*, 146811. [CrossRef]

Disclaimer/Publisher's Note: The statements, opinions and data contained in all publications are solely those of the individual author(s) and contributor(s) and not of MDPI and/or the editor(s). MDPI and/or the editor(s) disclaim responsibility for any injury to people or property resulting from any ideas, methods, instructions or products referred to in the content.